Electrically pumped continuous-wave vertical-cavity surface-emitting lasers at 2.6 μm

Shamsul Arafin, Alexander Bachmann, Kaveh Kashani-Shirazi, and Markus-Christian Amann

Citation: Applied Physics Letters **95**, 131120 (2009); doi: 10.1063/1.3240406
View online: http://dx.doi.org/10.1063/1.3240406
View Table of Contents: http://scitation.aip.org/content/aip/journal/apl/95/13?ver=pdfcov
Published by the AIP Publishing

Electrically pumped continuous-wave vertical-cavity surface-emitting lasers at ~2.6 μm

Shamsul Arafin,[a] Alexander Bachmann, Kaveh Kashani-Shirazi, and Markus-Christian Amann
Walter Schottky Institut, Technische Universität München, D-85748 Garching, Germany

(Received 13 July 2009; accepted 5 September 2009; published online 2 October 2009)

In this paper, electrically pumped GaSb-based vertical-cavity surface-emitting lasers operating continuous wave at a record long emission wavelength of ~2.6 μm are presented. Owing to the excellent thermal heat management, the devices exhibit single-mode operation up to a heat-sink temperature of 55 °C. Lateral current confinement and index guiding in the device are accomplished by utilizing the buried tunnel junction concept. Devices with aperture diameters of 6 μm show maximum output powers of 0.3 mW at room temperature with quantum efficiencies around 10%. © *2009 American Institute of Physics*. [doi:10.1063/1.3240406]

Recently, there has been an increasing interest in midinfrared (mid-IR) diode lasers based on the (AlGaIn)(AsSb) material system on GaSb substrates due to a wide range of emerging applications. In particular, these lasers are currently of great interest for IR countermeasures against heat-seeking missiles in the military field,[1,2] thermal imaging systems,[3] chemical process monitoring,[4,5] and free-space optical communication.[6] In addition, in recent years, trace-gas sensing by tunable diode laser absorption spectroscopy (TDLAS) has also drawn lots of attention for security and environmental reasons.[7] Compared to conventionally used electrochemical cells, this method offers certain advantages for the study of absorption spectra of gaseous molecules since it significantly increases the gas detection sensitivity and selectivity.[8] Principally suited light sources are edge emitting, distributed feedback lasers, and vertical-cavity surface-emitting lasers (VCSELs). However, TDLAS requires a single-longitudinal and transverse-mode emission, high (electro)thermal wavelength tunability, and a cost-effective production.[9] Since VCSELs fulfill all these requirements, they can be considered as ideal laser sources for this gas sensing application.

The wavelength range from 2 to 4 μm is particularly interesting for TDLAS because a number of polluting gases exhibit strong absorption lines in this spectral region. Over the past couple of years, significant progress has been made toward the development of mid-IR (2–4 μm) semiconductor lasers. Bewley *et al.*[10,11] have already reported optically pumped Sb-based VCSELs at 2.9 μm for chemical sensing. Recently, monolithic electrically pumped (EP) GaSb-based multimode VCSELs in pulsed operation emitting at 2.63 μm have been obtained, which is the longest wavelength ever reported for any EP-VCSELs.[12] However, lasers with single-mode continuous wave (cw) emission are usually required, especially in absorption spectroscopy.

In this paper, we demonstrate the extension of GaSb-based buried tunnel junction (BTJ)-VCSEL technology to ~2.6 μm and present EP devices with maximum cw operation beyond room temperature (RT). This result was obtained using a simple and low-cost device fabrication. A schematic cross-section of the 2.6 μm GaSb-based VCSEL design is illustrated in Fig. 1.

Utilizing a twofold epitaxial growth process, the VCSEL structure was grown with a Varian Mod Gen II-MBE system equipped with solid sources and valved cracker cells for arsenic and antimony. The first epitaxial run starts with the growth of a bottom *n*-doped distributed Bragg reflector (DBR) consisting of 24 pairs of $AlAs_{0.09}Sb_{0.81}/GaSb$ layers. The calculated reflectivity of this mirror is approximately 99.7% at 2.6 μm, which is limited by free-carrier absorption. Thus, increasing the number of mirror pairs will not increase the reflectivity further. Then, the active region is deposited consisting of seven 10 nm thick quantum wells made of $Ga_{0.57}In_{0.43}As_{0.15}Sb_{0.85}$ with a compressive strain of 1.7%. The wells are separated by 8 nm thick GaSb barriers.

The first epitaxial growth is finished by the heavily doped tunnel junction layers made of n^+-InAsSb/p^+-GaSb, both doped with Si, which define the active area of the device (diameter, *D*) after structuring by conventional UV lithography and subsequent etching. Then, an *n*-doped current spreading layer and a highly doped n^+-InAsSb contact layer are deposited in the second epitaxial run. The top dielectric mirror consists of four pairs of evaporated SiO_2/a-Si. The reflectivity of this mirror is calculated to be 99.8% at 2.6 μm, i.e., slightly higher than the bottom mirror reflec-

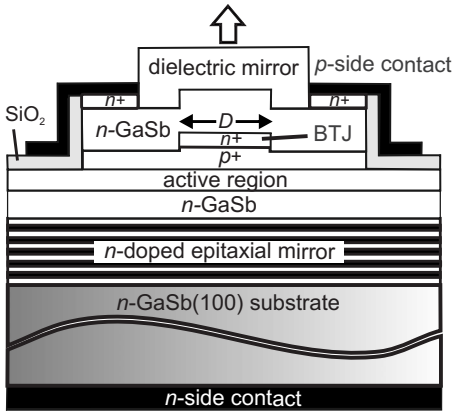

FIG. 1. Schematic cross-sectional view of a top-emitting 2.6 μm VCSEL structure. *D* is the active diameter defined by the BTJ.

[a]Electronic mail: arafin@wsi.tum.de. URL: http://www.wsi.tum.de.

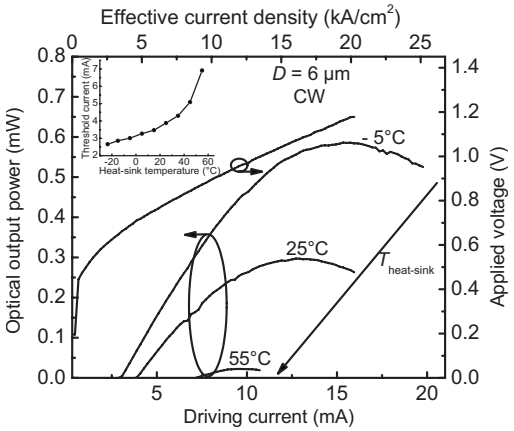

FIG. 2. Temperature dependent *LI*-characteristics of 2.6 μm BTJ-VCSEL. The *IV* curve is shown only for RT. Threshold current against heat-sink temperature is shown as inset.

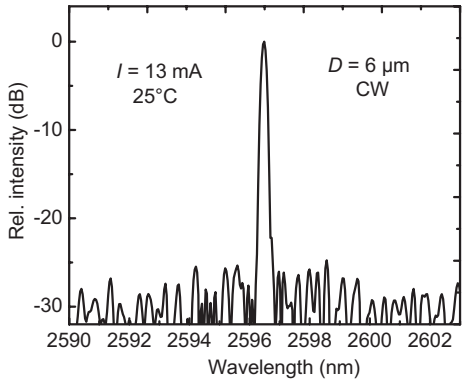

FIG. 3. Optical output spectrum showing an emission wavelength around 2596 nm.

tivity. Details of the GaSb-based BTJ-VCSEL fabrication process can be found elsewhere.[13]

The temperature dependent light-current (*L-I*) characteristics of a device with $D=6$ μm are presented in Fig. 2. The device shows cw operation up to 55 °C heat-sink temperature. The rollover peak power of this device obtained at RT (i.e., 25 °C) is 0.3 mW, yielding a differential quantum efficiency of 9.6%. At RT, the threshold current, I_{th} is 3.9 mA, corresponding to an effective threshold current density of around 5 kA/cm^2, where lateral carrier diffusion of 2 μm (as simulated) on each side of the BTJ is taken into account. This diffusion process leads to a broadening of the effectively pumped area in the active region. With respect to the corresponding photon energy at 2.6 μm wavelength ($\approx$0.48 eV), the threshold voltage is 240 mV higher.

The differential series resistance, R_s, is around 36 Ω at rollover current. Several parts of the device contribute to R_s, for instance, top *p*-contact, lateral spreading resistance by top *n*-GaSb layer, tunnel junction and bottom *n*-doped epitaxial mirror. The latter is dominating in such devices, despite the fact that the current spreads out in the bottom mirror. Here, the top *p*-contact,[14] the top lateral current spreading layer for the annular contact,[15] and the tunnel junction[16] contribute by about 0.9, 5.6, and 9.2 Ω, respectively, to the total calculated resistances. Therefore, the rest of the total series resistance can be attributed to the epitaxial bottom mirror.

The dependence of the threshold current as a function of the heat-sink temperature is displayed in the inset of Fig. 2. $I_{th}(T)$ characteristics in VCSELs is a bit complicated, which is determined by several factors, such as relative position of the gain peak with respect to the cavity mode, the change of the gain peak height caused by the spectral broadening, the effective differential gain value under device operating condition, and the temperature dependent loss mechanisms. It should be noted that the gain maximum should be negatively detuned with respect to the cavity mode in a way that the threshold minimum comes at RT under device operating condition. But this is not the case in Fig. 2 inset hinting that the designed offset value is not sufficient. Therefore, improvement of $I_{th}(T)$ characteristics, higher output power and higher temperature operation in the device can be obtained by a further blueshift of the emission of the active region or redshift of the cavity resonance by larger cavity length, i.e., increasing the offset value, which is rather a critical design issue.

The emission spectrum of a 6 μm device at RT in cw operation is shown in Fig. 3. The lasing wavelength is around 2596 nm and sidemode suppression ratio is measured over 27 dB.

The thermal tunability and the electrical power tunability of the lasers were measured by varying the heat-sink temperature at constant electrical power and by varying the laser current at constant heat-sink temperature, respectively, as illustrated in Fig. 4. High tuning rates are very attractive for gas sensing applications since several gas absorption lines may be scanned at a time by the temperature and current-induced self-heating effect. Note that the devices remain single-mode across their entire operating temperature and applied electrical power ranges.

The thermal properties of the presented VCSEL with 6 μm BTJ diameter have been studied by means of finite element analysis using a two-dimensional cylinder model. The commercial simulation program QUICKFIELD 5.4 (Ref. 17) was used. For simplicity, we assumed that all of the heat was generated in the active region. The heat power generation per unit volume q in the active region can be represented by the following relationship,

$$q = \frac{IV - P}{v},$$

where I is the laser driving current, V the voltage drop across the device, v the active region volume, and P the light output power. Thus, the temperature distribution of the device is obtained as shown in Fig. 5. The maximum temperature rise ΔT in the active region against the heat-sink temperature can be described by the thermal resistance

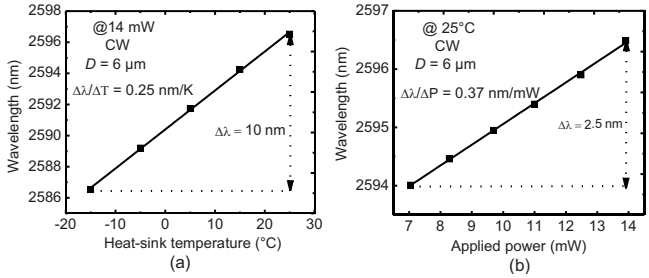

FIG. 4. Wavelength tuning by temperature at constant 14 mW of electrical power (a) and by electrical power at 25 °C (b), respectively.

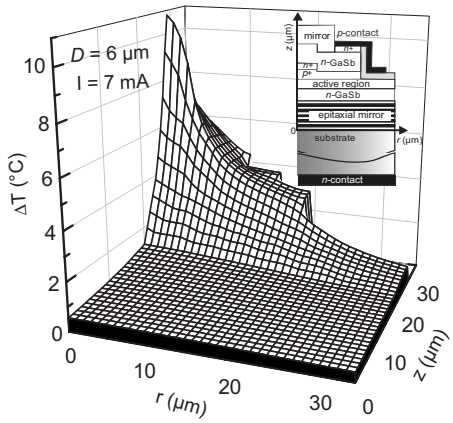

FIG. 5. Temperature distribution in the BTJ-VCSEL.

$$R_{\mathrm{th}} = \frac{\Delta T}{\Delta P_{\mathrm{electric}} - \Delta P_{\mathrm{optic}}} \approx \frac{\Delta T}{\Delta P_{\mathrm{electric}}} \times (\mathrm{if}\ \Delta P_{\mathrm{electric}} \gg \Delta P_{\mathrm{optic}}).$$

Thus, R_{th} is calculated to be 1700 K/W which demonstrates a better thermal management of the device than any InP-based[18] or GaSb-based[13] VCSELs with the same aperture reported so far. This value also shows a fair agreement with our experimental value

$$R_{\mathrm{th}} = \frac{\Delta\lambda}{\Delta P} \Big/ \frac{\Delta\lambda}{\Delta T} = 1480\ \ \mathrm{K/W}.$$

In conclusion, we have described a GaSb-based VCSEL with an emission wavelength of 2.6 μm using the BTJ technology. The EP devices show cw operation and single-mode emission up to a heat-sink temperature of 55 °C, which is expected to be increased further by an optimized mode-gain offset. Further improvements of the device performance are expected through an improved layer thickness control in the epitaxial growth, a better thermal management and an optimization of the relative alignment of the cavity mode and material gain peak.

This work has been financially supported by the European Union via NEMIS (Contract No. FP6-2005-IST-5-031845), the German Federal Ministry of Education and Research via NOSE (Contract No. 13N8772) and the German Excellence Cluster "Nanosystems Initiative Munich (NIM)."

[1]D. W. Stokes, L. J. Olafsen, W. W. Bewley, I. Vurgaftman, C. L. Felix, E. H. Aifer, J. R. Meyer, and M. J. Yang, J. Appl. Phys. **86**, 4729 (1999).
[2]A. Salhi, Y. Rouillard, A. Perona, P. Grech, M. Garcia, and C. Sirtori, Semicond. Sci. Technol. **19**, 260 (2004).
[3]G. Tessier, A. Salhi, Y. Rouillard, F. Genty, J. P. Roger, F. Montel, and D. Fournier, J. Phys. IV **125**, 375 (2005).
[4]P. Werle, Spectrochim. Acta, Part A **52**, 805 (1996).
[5]P. Werle and A. Popov, Appl. Opt. **38**, 1494 (1999).
[6]M. Yin, A. Krier, S. Krier, R. Jones, and P. Carrington, Proc. SPIE **6399**, 63990C.1 (2006).
[7]V. Ebert, Laser Appllications to Chemical, Security and Environmental Analysis LACSEA, Nevada, USA, 2006 (unpublished).
[8]J. Wagner, Ch. Mann, M. Rattunde, and G. Weimann, Appl. Phys. A: Mater. Sci. Process. **78**, 505 (2004).
[9]J. Chen, A. Hangauer, R. Strzoda, and M.-C. Amann, Appl. Phys. Lett. **91**, 141105 (2007).
[10]W. W. Bewley, C. L. Felix, I. Vurgaftman, E. H. Aifer, L. J. Olafsen, J. R. Meyer, L. Goldberg, and D. H. Chow, Appl. Opt. **38**, 1502 (1999).
[11]W. W. Bewley, C. L. Felix, I. Vurgaftman, E. H. Aifer, J. R. Meyer, L. Goldberg, J. R. Lindle, D. H. Chow, and E. Selvig, IEEE Photonics Technol. Lett. **10**, 660 (1998).
[12]A. Ducanchez, L. Cerutti, P. Grech, F. Genty, and E. Tournié, Electron. Lett. **45**, 265 (2009).
[13]A. Bachmann, K. Kashani-Shirazi, S. Arafin, and M.-C. Amann, IEEE J. Sel. Top. Quantum Electron. **15**, 933 (2009).
[14]S. Arafin, A. Bachmann, K. Kashani-Shirazi, S. Priyabadini, and M.-C. Amann, IET Optoelectron. (to be published).
[15]W. Nakwaski, M. Osinksi, and J. Cheng, Appl. Phys. Lett. **61**, 3101 (1992).
[16]O. Dier, C. Lauer, and M.-C. Amann, Electron. Lett. **42**, 419 (2006).
[17]http://www.quickfield.com/allnews/qf54release.htm, version 5.4 by Tera Analysis Ltd., CA.
[18]M. Ortsiefer, R. Shau, G. Böhm, F. Köhler, and M.-C. Amann, Appl. Phys. Lett. **76**, 2179 (2000).